Cent. Eur. J. Phys. • 11(9) • 2013 • 1091-1098
DOI: 10.2478/s11534-012-0140-x

VERSITA

Central European Journal of **Physics**

Above-threshold ionization of hydrogen and hydrogen-like ions by X-ray pulses

Research Article

Henri Bachau[1]*, Olimpia Budriga[2], Mihai Dondera[3†], Viorica Florescu [3‡]

1 *Centre des Lasers Intenses et Applications, Université Bordeaux I-CNRS-CEA, FR-33405 Talence, France*

2 *National Institute for Laser, Plasma and Radiation Physics, RO-077125 Bucharest-Măgurele, Romania*

3 *Faculty of Physics and Centre for Advanced Quantum Physics, University of Bucharest, RO-077125 Bucharest-Măgurele, Romania*

Received Apr 02, 2012; accepted Sep 21, 2012

Abstract: This paper adresses the problem of above-threshold ionization (ATI) of hydrogen interacting with an intense X-ray electromagnetic field. Two approaches have been used. In the first approach, we calculate generalized differential and total cross sections based on second-order perturbation theory for the electron interaction with a monochromatic plane wave, with the $\mathbf{A}^2$ and $\mathbf{A}\cdot\mathbf{P}$ contributions from the nonrelativistic Hamiltonian (including retardation) treated exactly. In the second approach, we solve the time-dependent Schrödinger equation (TDSE) for a pulsed plane wave using a spectral approach with a basis of one-electron orbitals, calculated with L^2-integrable B-spline functions for the radial coordinate and spherical harmonics Y_{lm} for the angular part. Retardation effects are included up to $O(1/c)$, they induce extra terms forcing the resolution of the TDSE in a three dimensional space. Relativistic effects [of $O\left(1/c^2\right)$] are fully neglected. The isoelectronic series of hydrogen is explored in the range $Z = 1 - 5$ in both TDSE and perturbative approaches. Photoelectron angular distributions are obtained for photon energies of 1 keV and 3 keV for hydrogen, and photon energy of 25 keV for the hydrogenic ion B^{4+}. Perturbative and TDSE calculations are compared.

PACS (2008): 32.80.rm, 32.80.Fb, 32.30.Rj

Keywords: Multiphoton ionization • X-ray • Above threshold ionization • Hydrogen• hydrogenic ions

*E-mail: bachau@celia.u-bordeaux1.fr
†E-mail: don@baratu.fizica.inibuc.ro
‡E-mail: flor@baratu.fizica.inibuc.ro

1. Introduction

The emergence of X-ray free-electron lasers which produce radiation at increasing peak intensities [1, 2], motivates the theoretical interest for the study of the atomic ionization induced by multiphoton absorption in the extreme ultraviolet (EUV) and X-ray photon energy range. It is expected that new experimental results, like the re-

cent one realized on neon with a femtosecond kilovolt X-ray beam [3], will stimulate the development of theoretical approaches able to describe non-linear processes induced by short wavelength fields. Also, since X-ray fields likely ionize inner-shell electrons, it should be possible at high intensity to investigate multiple ionization of the core in complex atoms. Here, it is worth noting that, even at intensities of the order of the atomic unit $I_0 = 3.51 \times 10^{16}$ W cm^{-2}, lowest order perturbation theory applies since the ponderomotive energy U_p is much smaller than the photon energy in the X-ray regime [4]. In two recent papers we have investigated two-photon above-threshold ionization of hydrogen in lowest-order perturbation theory (LOPT) [5], and resolving the TDSE [6]. Our aim is to explore retardation effects in a photon energy domain which has received little attention until now, and to develop appropriate theoretical approaches.

With monochromatic radiation, the two-photon ionization of ground state hydrogen and hydrogenic ions (with nuclear charge Z), was, up to now, described in LOPT by: i) nonrelativistic equations in dipole approximation (DA); ii) nonrelativistic equations in which retardation was only partially included, iii) exact relativistic formalism. The total cross section was the most investigated. As in the case of photoeffect, retardation effects are expected to be more visible in the electron angular distribution than in the total cross section. The formalism i), leads to the precise calculations, see [7] for a review paper and [8] for recent calculations. The latter calculations cover the low frequencies range, *i.e.*, from 10 nm to 90 nm. Details on the approaches ii), adopted in [5] and [9] in LOPT and in [6] in TDSE, will be discussed here. The full relativistic treatment [10] uses the partial wave expansion of the relativistic Green function and of the final electron continuum bispinor, and also the multipolar expansion of the radiation field. Details can be found in [11], as well as calculations of angular distribution for atomic number Z=1, 54 and 92. The approach involves complicated analytic and numerical developments, see [11]. The nondipole form of the light-atom interaction has received considerable attention in the UV domain; an illustrative example is the study of atomic stabilization (see [12], and references therein). We also note the pioneering work of Klarsfeld [13] and Gavrila [14, 15] (for Compton scattering), who calculated two-photon processes in the hydrogenic atom using a non-relativistic approach, including retardation effects; analytical developments presented in [15] will be used here.

For low atomic number Z, and in the EUV and X-ray ranges, it makes sense to use the nonrelativistic equations, including retardation, and not the full relativistic results. In a recent paper, we have investigated the absorption of two identical photons from the ground state of hydrogen [5], in second-order perturbation theory, in which the $\mathbf{A}^2$ term in the non-relativistic Hamiltonian is treated exactly, while the $\mathbf{A}.\mathbf{P}$ contribution is treated in DA. Total generalized cross sections, have been calculated for photon energies ranging from 13.7 eV to 50 keV. In the present work, both $\mathbf{A}^2$ and $\mathbf{A} \cdot \mathbf{P}$ terms include retardation effects (we calculate generalized total and differential cross sections), and the treatment is based on compact analytic expressions. Note that our development allows us to identify which contributions from the different terms in the Hamiltonian are sensitive to retardation effects. Besides, total cross section electron angular distributions will also be calculated. The results will be compared with a non-perturbative approach recently published [6], where retardation effects are included up to $O(1/c)$. In this approach we directly solve the time-dependent Schrödinger equation (TDSE) for a pulsed plane wave using a spectral method. Assuming a perturbative regime (*i.e.*, the two-photon ionization probability is proportional to the pulse duration and varies quadratically with the intensity), cross sections can be evaluated from TDSE calculations, thus allowing a comparison with LOPT. The advantage of the TDSE approach, is that it can be extended to the case of high intensity fields; for example to study processes involving the absorption of more than two photons, or to explore the limit of validity of perturbation theory.

While the case of hydrogen was investigated in previous works [5, 6], we now investigate two-photon ionization of hydrogen and hydrogen-like ions for nuclear charges $Z = 2 - 5$. In dipole approximation and nonrelativistic theory, it can be shown that scaling the photon energy, pulse duration, and laser intensity like Z^2, Z^{-2}, and Z^6, respectively, the ionization probability should remain constant along the isoelectronic series of hydrogen and the associated two-photon ionization cross section should scale like Z^{-6} [16, 17]. Therefore, any deviation from the scaling low can be attributed to retardation effects. Furthermore, checking that the calculations follow the scaling law in DA is a test for our calculations. Comparing LOPT and TDSE results, we discuss the validity of the approximation used in the TDSE approach. Finally, we compare electron angular distributions calculated for hydrogen and B^{4+}.

In the following section, we present the theoretical approach; we briefly recall the LOPT and TDSE approaches, details can be found in [5, 6]. Results are presented in Section 3. The conclusion is given in Section 4.

Atomic units (a.u.) are used throughout this paper unless otherwise stated.

2. Theory

Our calculations start with the nonrelativistic Hamiltonian for a one electron atom in the external electromagnetic field:

$$\mathcal{H} = \frac{1}{2}[\mathbf{P} + \mathbf{A}(\mathbf{r}, t)]^2 - \Phi(\mathbf{r}, t) + V(r)\,, \qquad (1)$$

where $\mathbf{A}(\mathbf{r}, t)$ and $\Phi(\mathbf{r}, t)$ are the vector and scalar potentials, respectively. The atomic potential $V(r)$ is assumed to be a central one. The electromagnetic field considered here is an idealized radiation pulse, namely a linearly polarized plane wave with a finite spatial extension in its propagation direction. We work in the Coulomb gauge ($\Phi = 0$, $\nabla \cdot \mathbf{A} = 0$).

2.1. Perturbative approach

In the case of a hydrogen-like atom with a fixed nucleus of charge Z, the expression of the two-photon ionization amplitude coming from second order perturbation theory, with retardation included is

$$\begin{aligned} M_{\rm NR}^{\rm ret} \;=\; & \langle\, E\,\mathbf{n}- \mid e^{2i\boldsymbol{\kappa}\cdot\mathbf{r}}\,\mathbf{s}^2 - 2e^{i\boldsymbol{\kappa}\cdot\mathbf{r}} \\ & \mathbf{s}\cdot\mathbf{P}\; G(E_1 + \omega + i\epsilon) \\ & \mathbf{s}\cdot\mathbf{P}\; e^{i\boldsymbol{\kappa}\cdot\mathbf{r}} \mid E_1\,\rangle\;,\;\; \epsilon \to 0^+, \end{aligned} \qquad (2)$$

where E_1 denotes the initial electron energy in hydrogenic state $1s$, $\boldsymbol{\kappa}$ the photon momentum, ω its energy, and G the Coulomb Green's function. The emitted electron has an energy E and an asymptotic direction characterized by the unity vector $\mathbf{n}$; the corresponding energy eigenfunction $\langle\,\mathbf{r} \mid E\,\mathbf{n}-\,\rangle$ is normalized on the energy and solid angle scales and it has the ingoing asymptotic behavior. The polarization vector of the photon $\mathbf{s}$ is normalized as $\mathbf{s}^*\cdot\mathbf{s} = 1$; it is real for linear polarization, otherwise it is complex. Here we consider linear polarization.
The ejected electron energy E is

$$E = E_1 + 2\omega\,, \qquad \omega \geq \frac{\mid E_1 \mid}{2}\,, \qquad E_1 = \frac{-Z^2}{2}, \qquad (3)$$

The two-photon absorption threshold $E_{2\gamma}$, is half of the photoelectric threshold $\mid E_1 \mid$. For light elements, this nonrelativistic threshold is low (it reaches 1.06 keV for Z=13), so the absorption of two photons in the low energy range is well described in DA. For photon energies ranging from the two-photon to the one-photon ionization thresholds, ionization is energetically possible only through the absorption of at least two photons. Above the second threshold, one photon and two photon ionization are both possible.

In DA, the contribution of the first term in the matrix element given in Eq. (2) (*i.e.*, the $\mathbf{A}^2$ contribution, called the sea-gull term in the literature of Compton scattering) vanishes. The absorption of low energy photons has been described in the literature by using the second term in Eq. (2), taken in DA.
In order to cover the higher energy regime, Varma *et al.* [9] have introduced a non-relativistic approach in which the first term is treated exactly and the second one in DA. A further approximation was done in the $\mathbf{A}\cdot\mathbf{P}$ term. Our recent numerical calculation [5], performed with the same starting point as in [9], revealed that, for the hydrogen atom, the term $\mathbf{A}^2$ has a negligible contribution up to photon energies of 50 keV.
In the present calculations, for the transition amplitude, we use the analytic results written in [15]. As they are valid for Compton scattering and we are interested in the absorption of two photons having the same momentum $\boldsymbol{\kappa}$, we have to use $-\boldsymbol{\kappa}_2 = \boldsymbol{\kappa}_1 = \boldsymbol{\kappa}$ in Gavrila's equations (in the case of radiation scattering $\boldsymbol{\kappa}_1$ is the absorbed photon momentum and $\boldsymbol{\kappa}_2$ the emitted photon momentum).
The structure of the transition amplitude in its dependence of photon polarization is the same as in Eq. (6) of [5], only the invariant amplitudes in the second term are different.

$$M_{\rm NR}^{\rm ret} \;=\; M_{\mathbf{A}^2} + M_{\mathbf{A}\cdot\mathbf{P}}^{\rm ret} \qquad (4)$$

$$M_{\mathbf{A}^2} \;=\; O^{\rm abs-two}\,\mathbf{s}^2,$$

$$M_{\mathbf{A}\cdot\mathbf{P}}^{\rm ret} \;=\; -2\left[\,P^{\rm ret}\,\mathbf{s}^2 + T^{\rm ret}\,(\mathbf{s}\cdot\mathbf{n})^2\,\right]. \qquad (5)$$

The amplitude denoted by $O^{\rm abs-two}$ is obtained from the quantity $\mathcal{O}^{\rm abs-two}$ in [5], multiplied by an appropriate conversion factor. For the last one we make use in Eqs. (B2-B3) and (A7) of the cited reference. The other amplitudes denoted with capital letters here, $P^{\rm ret}$ and $T^{\rm ret}$ are obtained from the amplitudes $\mathcal{P}$ and $\mathcal{T}$ given by Eqs. (48) and (52) of [15] (multiplied by an appropriate conversion factor), respectively, through the change of momenta mentioned before.
In order to calculate the generalized differential cross section in cm^4 s/sr, we use the general formula

$$\frac{d\sigma_{\rm NR}^{\rm ret}}{d\Omega_{\mathbf{n}}} = 2\pi^{N+1}\,\alpha^N\,a_0^{2N}\,\tau_0^{N-1}\,E_{ph}^{-N}\mid M_{\rm NR}^{\rm ret}\mid^2, \qquad (6)$$

where N is the number of photons absorbed (here $N = 2$), a_0 is given in cm and corresponds to the atomic unit of length, while τ_0 is given in s and corresponds to the atomic unit of time. E_{ph} is the photon energy in Rydbergs and $M_{\rm NR}^{\rm ret}$ is the two-photon amplitude in a.u. (see Eq. (2) for $N = 2$). The total cross section, in cm^4 s, is obtained by integrating the differential cross section given in Eq. (6)

over the electron emission solid angle $\Omega_{\mathbf{n}}$. In the generalized differential cross section we distinguish three contributions,

$$d\sigma_{\mathrm{NR}}^{\mathrm{ret}} = d\sigma_{\mathbf{A}^2} + d\sigma_{\mathbf{A}\cdot\mathbf{P}}^{\mathrm{ret}} + d\sigma_{\mathrm{interf}} \,. \tag{7}$$

2.2. Non-perturbative approach

Details about the procedure used to resolve the TDSE have been presented in a recent paper [6], here we only recall the main steps of the approach. We first introduce the TDSE for the system atom+field and the approximation applied to describe the nondipole corrections. Then we give some details about TDSE calculations, followed by the formulas used to extract the photoelectron distributions.
The TDSE reads

$$i\frac{\partial}{\partial t}\psi(\mathbf{r},t) = \mathcal{H}\psi(\mathbf{r},t) \tag{8}$$

where $\mathcal{H}$ is given in Eq. (1) and $\psi(\mathbf{r},t)$ is the wave function solution of the system. The pulse is described with the help of the vector potential

$$\mathbf{A}(\mathbf{r},t) = A\left(t'\right)\,\mathbf{e_z}\,, \tag{9}$$

where $t' \equiv t - x/c = t - \alpha x$, with α the fine structure constant. The function $A(t')$ has to be non vanishing on a finite interval of the independent variable t', of width denoted τ (*i.e.*, the total pulse duration) in the following. Given the form (9) for the pulse, the Hamiltonian (1) becomes

$$\mathcal{H} = \frac{1}{2}\mathbf{P}^2 + V + A\left(t'\right)\,P_z + \frac{1}{2}\,A^2\left(t'\right)\,. \tag{10}$$

Here, it is worth recalling that the numerical integration of the corresponding TDSE is too demanding if we want to treat exactly the retardation effect since, unlike in the case of dipole approximation, we have to solve a true 3D problem, with further complications due to the term $A(t-\alpha\,x)\,P_z$, difficult to evaluate in any representation of the wave function. In order to build a Hamiltonian more adapted to the practical constraints and consistent with the nonrelativistic approximation, we follow here a procedure which is close to that presented in paper [18] (used in the latter paper to describe the magnetic field effect on stabilization). Supposing that the region of small distances gives the dominant contribution to the response of the atom exposed to the X-ray pulse, it is justified to approximate the function $A(t-\alpha x)$ by its truncated power series in x. The simplest approximation, used in this paper, is

$$A\left(t'\right) \approx A(t) - \alpha\dot{A}(t)\,x = A(t) + \alpha F(t)x\,, \tag{11}$$

where $F(t) \equiv -\dot{A}(t)$. The quality of this approximation depends on both the values of the x coordinate and on the X-ray pulse characteristics. In particular, for a not too short pulse with a central photon frequency ω, and values of x around 1 a.u. (in the case of hydrogen), the necessary condition of validity is $\alpha\,\omega < 1$ or, equivalently, $\omega < 3.73$ keV. For an hydrogenic ion of charge Z (with a radius about $1/Z$), the latter condition reads: $\alpha\,\omega < Z$.
With the approximation (11) the Hamiltonian is written

$$\mathcal{H} \approx \frac{1}{2}\mathbf{P}^2 + V + A(t)\,P_z + \alpha\,F(t)\,x\,P_z + \alpha\,F(t)\,A(t)\,x\,, \tag{12}$$

where we have ignored the term $A^2(t)/2$ (function of t only) and we have retained terms up to the first-order in α. It is to be mentioned that neglecting terms of the order $\alpha^2 = 1/c^2$ in Eqs. (11) and (12) is consistent with the nonrelativistic approximation - if we want to keep retardation terms of the order α^2 or higher, it is also necessary to include relativistic corrections. We rewrite Eq. (12) in the form

$$\mathcal{H} \approx H_a + \mathcal{H}_{DA}^{(1)} + \mathcal{H}_{RET}^{(1)} + \mathcal{H}_{RET}^{(2)}\,, \tag{13}$$

expressing the Hamiltonian as a sum of the atomic Hamiltonian $H_a \equiv \mathbf{P}^2/2 + V$, of the interaction term in dipole approximation $\mathcal{H}_{DA}^{(1)} \equiv A(t)\,P_z$, and of other two terms, describing non-dipole corrections: $\mathcal{H}_{RET}^{(1)} \equiv \alpha\,F(t)\,x\,P_z$ and $\mathcal{H}_{RET}^{(2)} \equiv \alpha\,F(t)\,A(t)\,x$. Within LOPT, the terms $\mathcal{H}_{DA}^{(1)} + \mathcal{H}_{RET}^{(1)}$ (related to $\mathbf{A}\cdot\mathbf{P}$) and $\mathcal{H}_{RET}^{(2)}$ (associated to $\mathbf{A}^2$) induce one and two-photon transitions, respectively. Note that one and two-photon transitions can be distinguished provided that the laser bandwidth is much smaller than the photon energy. In the case of a total pulse duration τ of 20 oscillations of the field, considered in the following section, the laser bandwidth is of the order of $2\pi/\tau = \omega/20$, therefore the latter condition is fulfilled.
For the numerical integration of TDSE corresponding to the approximate Hamiltonian (12), in the case of a central potential $V(r)$, we have used a spectral method based on the expansion of the wave function

$$\psi(\mathbf{r},t) = \sum_{n,l,m} e^{-iE_{nl}t}\,c_n^{(l,m)}(t)\,u_{nlm}(\mathbf{r}) \tag{14}$$

in a discrete basis of H_a eigenfunctions $\{u_{nlm}(\mathbf{r}) = X_{nl}(r)/r\,Y_{lm}(\mathbf{r}/r)\}$. The eigenvalues of H_a, indexed as E_{nl},

are determined together with the radial eigenfunctions $X_{nl}(r)$ by solving numerically the radial Schrödinger equation in a basis of B-spline functions [19]. In a typical calculation, we use 5 angular momenta l within the range $l = 0-4$, with $|m| \leq l$, and a basis of 1300 B-spline functions of order $k = 7$, distributed linearly inside a box of length $b = 200$ a.u. The box radius b is chosen such that the probability to find the photoelectron outside the box at the end of the pulse is negligible. The convergence of the calculations is checked by varying the box size and/or the number of basis functions and angular momenta. The functions $u_{nlm}(\mathbf{r})$ are normalized to 1. At $t = t_i$ (*i.e.*, at the beginning of the pulse) the system is in hydrogenic state $1s$; $\psi(\mathbf{r}, t_i) = \langle\, \mathbf{r} \mid E_1 \,\rangle$. The coefficients $c_n^{(l,m)}(t)$ satisfy a system of coupled equations, with couplings determined by the non-diagonal matrix elements of the Hamiltonian. Besides the couplings ($l' = l \pm 1$; $m' = m$), specific to DA (due to the term $\mathcal{H}_{DA}^{(1)}$), the last two terms of the Hamiltonian (13) introduce new couplings, not conserving the magnetic quantum number m: $\mathcal{H}_{RET}^{(1)}$ and $\mathcal{H}_{RET}^{(2)}$ couple, respectively, states with ($l' = l$, $l \pm 2$; $m' = m \pm 1$) and ($l' = l \pm 1$; $m' = m \pm 1$).

Once the wave function $\psi(\mathbf{r}, t)$ is known at the end of the pulse, the photoelectron distributions can be extracted from it. For the most detailed distribution, the energy and angular distribution, we use the formula

$$\mathcal{P}(E, \mathbf{n}) = k\, |\mathcal{A}(E, \mathbf{n})|^2 \,, \tag{15}$$

where $E = k^2/2$ and $\mathbf{n}$ have been previously defined (see Eq. (2)). The amplitude $\mathcal{A}(E, \mathbf{n})$, is obtained by projecting the wave function, at $t = t_f$ (*i.e.*, at the end of the pulse), onto the incoming continuum solutions

$$\mathcal{A}(E, \mathbf{n}) \equiv \langle\, k\, \mathbf{n} - \mid \psi(t_f) \,\rangle \,. \tag{16}$$

$\langle\, \mathbf{r} \mid k\, \mathbf{n} - \,\rangle$ is the eigenfunction associated with the emitted electron, it is equivalent to $\langle\, \mathbf{r} \mid E\, \mathbf{n} - \,\rangle$ previously defined but normalized on the momentum scale. Up to a non-essential phase factor, $\mathcal{A}(E, \mathbf{n})$ coincides with the photoionization amplitude, a quantity which determines the asymptotic behavior of the wave function after the end of the pulse (see for example [20]). The formulas giving the expression of the coefficients $\mathcal{A}_{lm}(k)$ of the expansion of $\mathcal{A}(E, \mathbf{n})$ in spherical harmonics $Y_{lm}(\mathbf{n})$, as well as some details about their numerical calculation and their form in LOPT are given in Appendix of [6].

Integrating $\mathcal{P}(E, \mathbf{n})$ given in Eq. (15), we find the photoelectron angular distribution

$$\mathcal{P}(\mathbf{n}) = \int k\, |\mathcal{A}(E, \mathbf{n})|^2 \, dE \,, \tag{17}$$

and the photoelectron energy spectrum

$$\mathcal{P}(E) = k \int |\mathcal{A}(E, \mathbf{n})|^2 \, d\Omega_{\mathbf{n}} = k \sum_{l,\, m} |\mathcal{A}_{lm}(k)|^2 \,. \tag{18}$$

The energy distribution can also be determined by the summation

$$\mathcal{P}(E) = \sum_{l,\, m} \mathcal{P}_{lm}(E) \,, \tag{19}$$

where the photoelectron partial spectrum $\mathcal{P}_{lm}(E)$ is calculated at energies coinciding to E_{nl}

$$\mathcal{P}_{lm}(E_{nl}) \approx \left| c_n^{(l,m)}(t_f) \right|^2 / \Delta E \,, \tag{20}$$

where $\Delta E \equiv (E_{n+1,\,l} - E_{n-1,\,l})/2$. Given the normalization of the function $u_{nlm}(\mathbf{r})$ to 1, mentioned above, the coefficient $1/\Delta E$ corresponds to the density of states [21]. An interpolation procedure, performed for each channel (l, m) in (19), leads to the evaluation of $\mathcal{P}(E)$.

Assuming a perturbative regime, cross sections can be evaluated from TDSE calculations. A simple relation can be established between the ionization probability P_N, extracted from TDSE resolution, and the associated cross section. For the absorption of N photons it reads,

$$\sigma_{tdse}^{ret}(N) = C(N) \left(\frac{\omega}{I} \right)^N \frac{P_N}{\tau} \,, \tag{21}$$

where the cross section is given in $\mathrm{cm}^{2N}\ \mathrm{s}^{N-1}$, the intensity I in $\mathrm{W\ cm}^{-2}$, the photon energy ω in joules, and the total pulse duration τ in seconds. $C(N)$ takes into account the effective pulse duration [17], which depends on the pulse envelope. For a $\cos^2$ pulse $C(1) = \frac{8}{3}$, $C(2) = \frac{128}{35}$ ...As a matter of fact, the differential cross sections can be obtained by replacing P_N with the appropriate density of probability in the above expression.

3. Results and discussion

In Tab. 1 we present LOPT calculations for the isoelectronic series of hydrogen, from $Z = 1$ to $Z = 5$. The photon energy scales as Z^2 and, as it is explained in the Introduction, we expect that the two-photon ionization cross section scales as Z^{-6} in non-relativistic and dipole approximations. It is easy to check that the cross section $\sigma_{\mathrm{NR}}^{\mathrm{da}}$ (last column in the Tab. 1) follows this law. Comparing the cross sections in dipole and non-dipole (fifth column) approximations, we note that they differ by less than 1% for $Z = 1$ but the relative difference increases with Z, it is close to 30% for $Z = 5$. Finally we have performed calculations neglecting $M_{\mathbf{A}^2}$ (or $M_{\mathbf{A}\cdot\mathbf{P}}^{\mathrm{ret}}$) in $M_{\mathrm{NR}}^{\mathrm{ret}}$ (see Eq. (4)). The

table shows (third and fourth columns) that the term $\mathbf{A}^2$ has a small contribution in the cross section, even when retardation effects are important. Therefore most of the retardation correction in the total cross section originates from the term $M^{\rm ret}_{\mathbf{A}\cdot\mathbf{P}}$.

In order to give a physical interpretation of the retardation effect, LOPT or TDSE can be used, but it is, in general, easier to extract the relevant information from LOPT. The two-photon transitions involving the coupling terms $\mathbf{A}^2$ and $\mathbf{A}\cdot\mathbf{P}$ are directly related to the first and second coupling terms in Eq. (4), respectively. Developing the Green operator in Eq. (4), it is easy to show that $\mathbf{A}\cdot\mathbf{P}$ first couples the intial state to intermediate states, $\mathbf{A}\cdot\mathbf{P}$ then couples the latter states to the final continuum (see Eq. (10) in [9]). We recall first that, considering the selection rule ($l' = l \pm 1$; $m' = m$) in DA and linear polarization, two-photon ionization from the ($l = 0, m = 0$) initial state can be interpreted as a first dipole transition to intermediate states ($l = 1, m = 0$) followed by a second dipole transition to ($l = 0, m = 0$) and ($l = 2, m = 0$) final states. When retardation is included, the latter channels dominate but the calculations show that the two-photon transitions also populate ($l = 3, |m| = 1$) and, to a lesser extent, ($l = 1, |m| = 1$) final states (see figure Fig. 1 in [6]). The channels leading to the dominant ($l = 3, |m| = 1$) state can be understood considering the coupling terms $\mathcal{H}^{(1)}_{DA} + \mathcal{H}^{(1)}_{RET}$ and $\mathcal{H}^{(2)}_{RET}$, associated to $\mathbf{A}\cdot\mathbf{P}$ and $\mathbf{A}^2$, respectively. We recall that $\mathcal{H}^{(1)}_{RET}$ and $\mathcal{H}^{(2)}_{RET}$ couple, respectively, states with ($l' = l,\ l \pm 2$; $m' = m \pm 1$) and ($l' = l \pm 1$; $m' = m \pm 1$). On the basis of the coupling rules, it is easy to show that the population of ($l = 3, |m| = 1$) originates from the term $\mathcal{H}^{(1)}_{DA} + \mathcal{H}^{(1)}_{RET}$. First the dipole transition populates the intermediate states ($l = 1, m = 0$) which are coupled to ($l = 3, |m| = 1$) states by the retardation term $\mathcal{H}^{(1)}_{RET}$. This term can also first populate the intermediate states ($l = 2, |m| = 1$) which are coupled to ($l = 3, |m| = 1$) final states through dipole transitions. It is worth noticing that the term $\mathcal{H}^{(2)}_{RET}$, corresponding to a two-photon transition, does not couple the initial ($l = 0, m = 0$) and final ($l = 3, |m| = 1$) states. The main effect of retardation is to lead to final states of different symmetry than the ones calculated with DA. Therefore, retardation effects are expected to increase the two-photon ionization total cross sections. Concerning the ($l = 1, |m| = 1$) final states, less populated than ($l = 3, |m| = 1$), the situation is more complex. There are in fact two channels leading to the population of ($l = 1, |m| = 1$) states; the first one involves combined couplings, as in the case of ($l = 3, |m| = 1$) states, in the second channel $\mathcal{H}^{(2)}_{RET}$ directly couples the initial ($l = 0, m = 0$) and final ($l = 1, |m| = 1$) states. The relative importance of the two channels can be visualized in Fig. 2 of [6]. These considerations explain why $\mathbf{A}^2$ has a small contribution in the cross section.

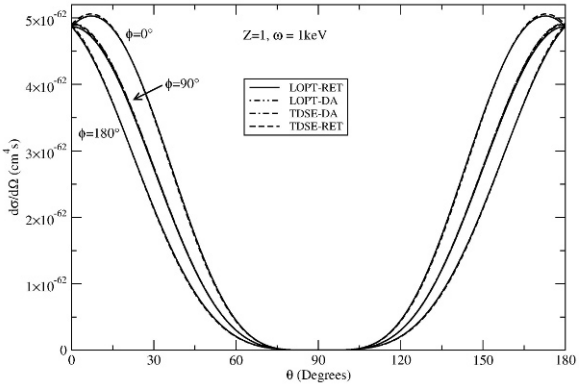

Figure 1. Angular distributions of photoelectrons (*versus* the polar angle θ) with energies corresponding to two-photon absorption. Three azimuthal angles are considered; $\phi = 0$, 90, 180 degrees. Calculations are performed in LOPT and TDSE approaches (indicated in the legend). Here $Z = 1$ and $\omega = 1$ keV. Note that the calculations in DA (LOPT-DA and TDSE-DA in the legend) perfectly overlap, this is also the case in other figures.

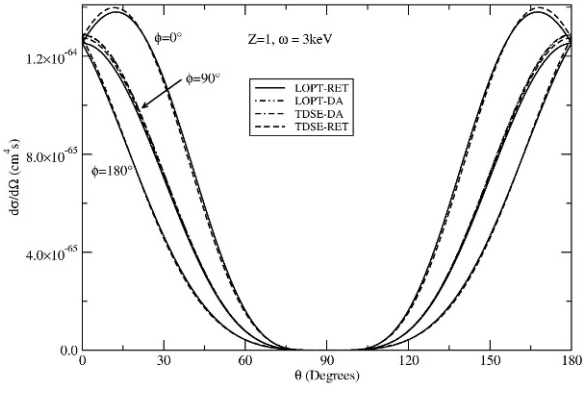

Figure 2. Angular distributions of photoelectrons (*versus* the polar angle θ) with energies corresponding to two-photon absorption. Three azimuthal angles are considered; $\phi = 0$, 90, 180 degrees. Calculations are performed in LOPT and TDSE approaches (indicated in the legend). Here $Z = 1$ and $\omega = 3$ keV.

TDSE results are presented in Tab. 2, and show the calculations performed within the dipole and non-dipole approximations. The laser parameters follow the Z-scaling laws (see table caption) leading in DA to a constant probability of ionization along the isoelectronic series [16, 17]. We note that the scaling law is perfectly verified (third column). We have calculated the two-photon ionization cross sections on the basis of Eq. (21), it is interesting to note that the cross sections are in rather good agreement with those calculated within LOPT (see Tab. 1). This

Table 1. The total cross sections calculated within LOPT, given in cm^4 s, for hydrogenic ion with nuclear charge Z. The photon energy is 1 keV for $Z = 1$ and it scales as Z^2 along the isoelectronic series. The cross section $\sigma_{\mathbf{A}\cdot\mathbf{P}}$ refers to calculation where $M_{\mathbf{A}\cdot\mathbf{P}}$ is neglected in Eq. (4). The cross section $\sigma_{\mathbf{A}^2}$ refers to calculation where $M_{\mathbf{A}\cdot\mathbf{P}}$ is neglected in Eq. (7). σ_{NR}^{da} is the two-photon total cross section calculated in dipole approximation. y-x indicates $y\,10^{-x}$.

Z	ω (keV)	$\sigma_{\mathbf{A}\cdot\mathbf{P}}$	$\sigma_{\mathbf{A}^2}$	σ_{NR}^{ret}	σ_{NR}^{da}
1	1	1.25-61	2.55-65	1.24-61	1.23-61
2	4	2.03-63	1.68-66	2.02-63	1.92-63
3	9	1.91-64	3.61-67	1.89-64	1.69-64
4	16	3.76-65	1.29-67	3.67-65	3.00-65
5	25	1.12-65	6.18-68	1.09-65	7.87-66

point is of particular importance considering that the approximation (11) sustaining the TDSE development is in principle valid for $\alpha\,\omega < Z$. It is easy to check that the latter inequality is strictly verified for $Z < 4$. Therefore, in practice, it seems that the validity of the approximation (11) extends to the domain where $\alpha\,\omega$ is of the order of Z. Finally we have checked that the term $\mathcal{H}_{RET}^{(1)}$ (related to $\mathbf{A}\cdot\mathbf{P}$ contribution) in Eq. (13) dominates the retardation corrections in the total ionization probability, in agreement with LOPT calculations.

In Fig. 1 we present two-photon ionization angular distributions for hydrogen and photon energy of 1 keV, for energies corresponding to the second peak in the electron spectrum ($E_1 + 1.5\,\omega < E < E_1 + 2.5\,\omega$). We have also excluded the ($l = 1, m = 0$) and ($l = 2, m = 1$) partial spectra which dominate in one-photon ionization [6] since they may have a non negligible contribution in the region of the second peak. In the figures, θ is the angle between the asymptotic electron momentum (characterized by the unity vector $\mathbf{n}$) and the polarization direction $\mathbf{e}_z$, and ϕ is the azimuthal angle formed with the propagation-polarization plane. We note a perfect agreement between LOPT and TDSE calculations. Due to retardation effects, the distributions at the azimuthal angles $\phi = 0$ and $\phi = 180$ degrees deviate from dipole approximation. At $\phi = 90$ degrees, LOPT and TDSE results cannot be distinguished in DA and the curve representing nondipole results practically coincides with the curve in dipole approximation [6]. Similar remarks can be made at 3 keV (see Fig. 2), but the retardation effects are stronger at this photon energy. Finally we show the case of $Z = 5$ and $\omega = 25$ keV in Fig. 3. As expected the agreement between LOPT and TDSE results, including retardation, is not as good as in the precedent cases (but they perfectly agree in DA), nevertheless the curves show similar behavior.

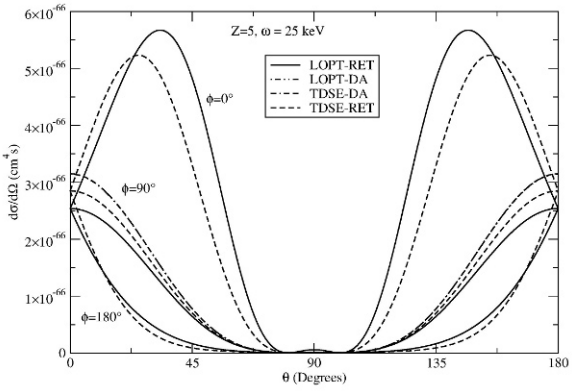

Figure 3. Angular distributions of photoelectrons (*versus* the polar angle θ) with energies corresponding to two-photon absorption. Three azimuthal angles are considered; $\phi = 0$, 90, 180 degrees. Calculations are performed in LOPT and TDSE approaches (indicated in the legend). Here $Z = 5$ and $\omega = 25$ keV.

4. Conclusion

We have investigated two-photon ionization of the hydrogen atom and hydrogenic ions with X-ray fields in the range $Z = 1 - 5$. Two methods have been developed: a perturbative approach based on second-order perturbation theory, and a non-perturbative one based on the resolution of the time-dependent Schrödinger equation. In LOPT an analytical expression is used for the amplitude associated to two-photon ionization. In TDSE we use an approximation for the interaction term, which is valid up to $O(1/c)$. In the case of a hydrogen atom with $\omega = 1$ keV, the results obtained in LOPT and TDSE agree very well, but the retardation effects in two-photon ionization total cross sections are very small (less than 1%). Following the hydrogen isoelectronic series with a photon energy scaling like Z^2, the retardation effects are more and more important; they introduce a difference of 30% with DA cross sections for $Z = 5$ and $\omega = 25$ keV. The retardation effects are mainly due to the interaction term $\mathbf{A}\cdot\mathbf{P}$; this

Table 2. Two-photon ionization probabilities and associated cross sections calculated with TDSE (see Eq. (21)). The cross section are expressed in cm^4 s and the labels da and ret stand for dipole and non-dipole approximation calculations, respectively. For $Z = 1$ we consider a photon energy ω of 1 keV, a pulse duration τ of 20 optical cycles and an intensity I of 10^{17} W cm^{-1}. Along the isoelectronic series, ω, τ and I scale as Z^2, Z^{-2} and Z^6, respectively. y-x indicates $y\,10^{-x}$.

Z	ω (keV)	P^{da}	σ^{da}_{tdse}	P^{ret}	σ^{ret}_{tdse}
1	1	1.085-12	1.23-61	1.10-12	1.24-61
2	4	1.085-12	1.92-63	1.13-12	2.00-63
3	9	1.085-12	1.69-64	1.18-12	1.84-64
4	16	1.085-12	3.01-65	1.26-12	3.49-65
5	25	1.085-12	7.88-66	1.36-12	9.89-66

has been checked in both LOPT and TDSE calculations. The latter calculations rely on an approximation valid, in principle, for $\alpha\,\omega < Z$, but there is reasonable agreement with LOPT beyond this condition. Regarding the angular distributions, the retardation effects are more pronounced than in the case of total cross sections. A clear deviation with DA is observed at azimuthal angles of 0 and 180 degrees, it increases with Z (and ω). More results in LOPT and in-depth analysis will be presented in a forthcoming paper [22].

Acknowledgments

This work has been supported by the European COST Action CM0702. O.B. thanks the support of the Ministry od Education and Research, Romania (program Laplas 3, PN 09 39).

References

[1] W. Ackermann et al., Nat. Photonics 1, 336 (2007)
[2] P. Emma et al., Nat. Photonics 4, 641 (2010)
[3] G. Doumy et al., Phys. Rev. Lett. 106, 083002 (2011)
[4] M. G. Makris, P. Lambropoulos, A. Mihelič, Phys. Rev. Lett. 102, 033002 (2009)
[5] V. Florescu, O. Budriga, H. Bachau, Phys. Rev. A 84, 033425 (2011)
[6] M. Dondera, H. Bachau, Phys. Rev. A 85, 013423 (2012)
[7] A. Maquet, V. Véniard, T. Marian, J. Phys. B-At. Mol. Opt. 31, 3743 (1998)
[8] E. Karule, A. Gailitis, J. Phys. B-At. Mol. Opt. 43, 065601 (2010)
[9] H. R. Varma, M. F. Ciappina, N. Rohringer, R. Santra, Phys. Rev. A 80, 054324 (2009)
[10] P. Koval, S. Fritzsche, A. Surzhykov, J. Phys. B-At. Mol. Opt. 36, 873 (2003)
[11] P. Koval, S. Fritzsche, A. Surzhykov, J. Phys. B-At. Mol. Opt. 37, 375 (2004)
[12] J. R. Vázquez de Aldana et al., Phys. Rev. A 64, 013411 (2001)
[13] S. Klarsfeld, Lett. Nuovo Cimento 2, 548 (1969)
[14] M. Gavrila, Lett. Nuovo Cimento 2, 180 (1969)
[15] M. Gavrila, Phys. Rev. A 6, 1348 (1972)
[16] W. Zernik, Phys. Rev. 135, A51 (1964)
[17] L. B. Madsen, P. Lambropoulos, Phys. Rev. A 59, 4574 (1999)
[18] H. G. Muller, In B. Piraux, K. Rzazewski (Ed.), Weakly relativistic stabilization: the effect of the magnetic field (Kluwer, Dordrecht, 2001) 339
[19] H. Bachau, E. Cormier, P. Decleva, J. E. Hansen, F. Martín, Rep. Prog. Phys. 64, 1815 (2001)
[20] M. Dondera, Phys. Rev. A 82, 053419 (2010)
[21] A. Macías, F. Martín, A. Riera, M. Yáñez, Int. J. Quantum Chem. 33, 279 (1988)
[22] V. Florescu, O. Budriga, H. Bachau, Phys. Rev. A 86, 033413 (2012)